Journal of Applied Mechanics and Technical Physics, Vol. 47, No. 4, pp. 492–504, 2006

SPECIAL AND EXTREME TRIPLE SHOCK-WAVE CONFIGURATIONS

V. N. Uskov and M. V. Chernyshov

UDC 533.6.011.72

Triple shock-wave configurations in steady supersonic flows of an inviscid perfect gas are considered. Triple configurations with special intensities of shock waves and extreme ratios of various flow parameters behind these configurations are determined.

Key words: *triple configuration, shock wave, special intensities, extreme ratios of parameters.*

1. Object of the Study. Formulation of the Problem. A triple configuration (TC) of shock waves is the structure of gas-dynamic discontinuities in a supersonic flow, which consists of three shock waves (j_i, where $i = 1, 2, 3$) and a tangential discontinuity τ possessing a common (triple) point T (Fig. 1). The initial-flow streamline that arrives at the triple point divides the flow into two parts, one of them passing through a system (sequence) of shock waves j_1 and j_2, and the other passing only through one (basic or resultant) shock wave j_3. The tangential discontinuity τ separates flows moving along it behind the shock waves j_2 and j_3; therefore, this tangential discontinuity is sometimes called the slip line.

The classification proposed by Landau [1] for discontinuities with respect to the point T allows us to consider the shock wave j_1 to arrive at the triple point. The flow behind the shock wave j_1 is supersonic if there is the next shock wave j_2, which can either arrive at the point T (Fig. 1a) or emanate from this point (Fig. 1c–e). In the case of a subsonic flow behind the shock waves j_2 (Mach number $M_2 < 1$) or j_3 ($M_3 < 1$), the directions of these shock waves in the vicinity of the point T do not allow us to state whether they are the reason for TC formation or the consequence of the latter.

TC calculation in a flow with a certain Mach number normally requires setting the parameters of the incoming shock wave j_1 (e.g., the angle of its inclination to the free stream σ_1 or intensity J_1, which is the ratio of static pressures ahead of the shock wave and behind it). TC formation is sometimes called the "branching" of the incoming shock wave. The triple configuration is determined by the following conditions of dynamic compatibility at the discontinuity: 1) equal static pressures ($p_2 = p_3$); 2) identical directions of flows separated by the discontinuity.

Thus, a continuous supersonic flow in the TC transforms to a discontinuous flow consisting of two flows with different gas-dynamic parameters f_2 and f_3 behind the TC, which are separated by a discontinuity. The ratios $I_f = f_2/f_3$ and the differences $\Delta\bar{f}_\tau = (f_2 - f_3)/f$ (f stands for flow parameters ahead of the triple point) characterize flow nonuniformity caused by different degrees of transformation of initial-flow parameters in a system of two shock waves and in a single basic shock wave. If the TC is formed in a nonuniform initial flow or the shock waves j_i are curved, the conventional conditions on the discontinuity τ are supplemented by differential conditions [1]: 1) equal curvature of the streamlines adjacent to the discontinuity τ; 2) equal derivatives of static pressure on the two sides of the discontinuity, which are taken along the discontinuity τ. In addition to the initial-flow nonuniformity, the solution of the problem is affected by interrelated curvatures of shock waves in the vicinity of the triple point.

Single shock waves and systems composed of such shock waves have special properties and can be optimal in terms of various criteria [2–5]. These special features should be expected to be manifested in the nonuniform flow behind the TC as well. This issue has not been considered in the literature, except for papers [6, 7], though it is important for applied problems of transonic and supersonic aerodynamics and for the theory of supersonic jet

Baltic State Technical University "Voenmekh," St. Petersburg 190005; uskov@peterlink.ru. Translated from Prikladnaya Mekhanika i Tekhnicheskaya Fizika, Vol. 47, No. 4, pp. 39–53, July–August, 2006. Original article submitted July 4, 2005; revision submitted September 16, 2005.

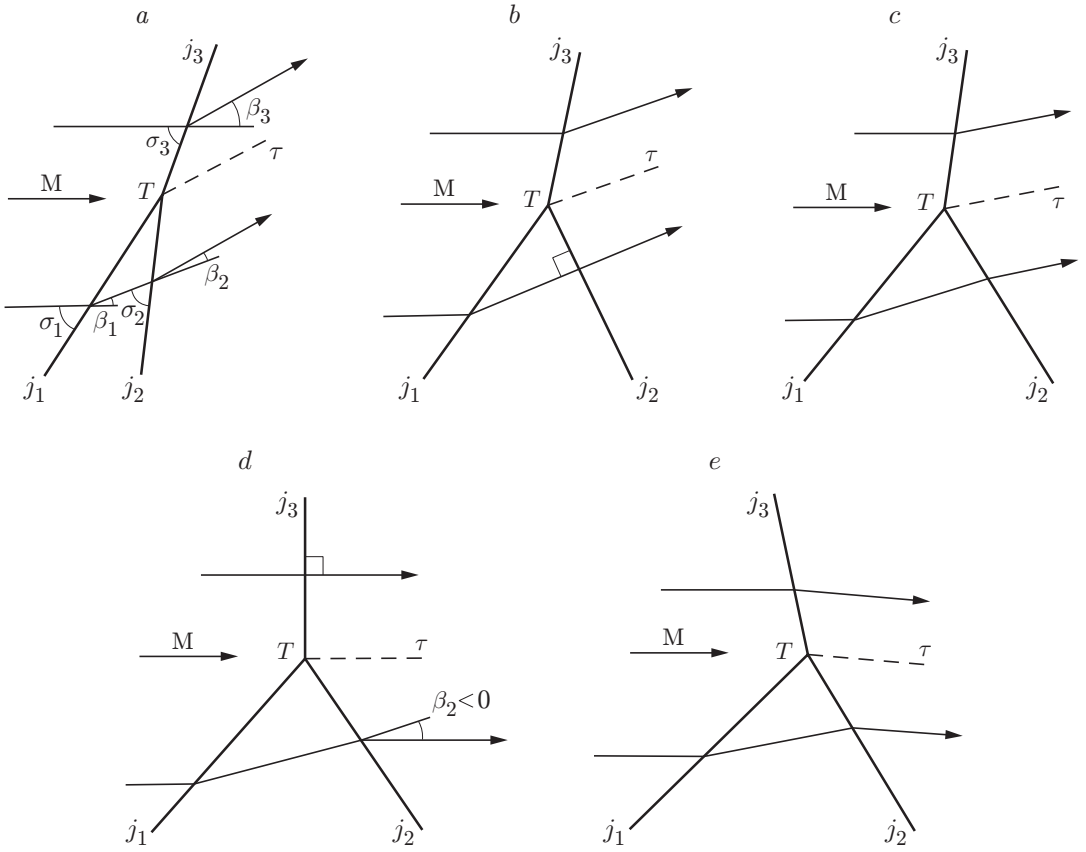

Fig. 1. Types of triple shock-wave configurations: (a) triple configuration of the third type; (b) triple configuration with the normal shock; (c) triple configuration of the second type; (d) steady Mach configuration; (e) triple configuration of the first type.

flows used in various engineering objects and technologies. Nonuniformity of flows, including those behind the TC, is often responsible for formation of separated and reverse flows, instabilities, self-induced oscillations, and strong acoustic fields, in particular, self-oscillatory regimes of interaction of supersonic jets with obstacles [7] and the flow around a blunted body with a spike [8]. Mixing of flows along the theoretical slip line (especially along the curved slip line) can lead to formation of strong vortices and even a reverse flow behind the Mach disk of a supersonic jet with the jet pressure ratio significantly different from unity.

The principle of motion reversibility allows us to use the theory of steady TCs in calculating similar structures of traveling shock waves [9] whose analysis is important in unsteady gas dynamics and physics of explosion.

The list of problems associated with calculation and analysis of triple configurations, which is far from being complete, shows that controlling the parameters of a nonuniform flow behind triple configurations is an urgent problem. The solution of this problem implies selecting of a certain intensity of the incoming shock wave j_1 (depending on the free-stream Mach number and on the ratio of specific heats γ), which would provide nonuniformity parameters $I_f(\mathrm{M}, \gamma, J_1)$ and $\Delta\bar{f}_\tau(\mathrm{M}, \gamma, J_1)$ necessary for solving this applied problem. The present paper described the analysis of special features and extreme values of parameters of flow nonuniformity behind the TC.

2. Governing Relations. The conditions of dynamic compatibility on the discontinuity τ relate the intensities J_i of the shock waves j_i, the flow Mach number ahead of the triple point, and the ratio of specific heats γ [1, 6, 10]:

$$J_1 J_2 = J_3; \tag{2.1}$$

$$\beta_1 + \beta_2 = \beta_3. \tag{2.2}$$

The intensity J_i of each shock wave is related to the angle of its inclination σ_i (see Fig. 1a) as

$$J_i = (1+\varepsilon)\mathrm{M}_k^2 \sin^2\sigma_i - \varepsilon,$$

where M_k is the Mach number ahead of the shock wave j_i and $\varepsilon = (\gamma-1)/(\gamma+1)$.

The angles β_i of flow deflection on the corresponding shock waves are determined by the intensities of these shock waves J_i and by the flow Mach numbers ahead of these shock waves:

$$|\beta_i| = \arctan\Big(\sqrt{\frac{(1+\varepsilon)\mathrm{M}_k^2 - \varepsilon - J_i}{J_i+\varepsilon}}\,\frac{(1-\varepsilon)(J_i-1)}{(1+\varepsilon)\mathrm{M}_k^2 - (1-\varepsilon)(J_i-1)}\Big).$$

The Mach number M_i behind the shock wave j_i is also determined by the Mach number ahead of this shock wave and by the intensity of the latter:

$$\mathrm{M}_i = \sqrt{\frac{(J_i+\varepsilon)\mathrm{M}_k^2 - (1-\varepsilon)(J_i^2-1)}{J_i(1+\varepsilon J_i)}}.$$

With the use of the relation $\Lambda_i = \ln J_i$, we can write condition (2.1) in the form

$$\Lambda_1 + \Lambda_2 = \Lambda_3, \tag{2.3}$$

which admits mapping of the shock wave j_i in the form of the vector (β_i, Λ_i) on the plane of shock-wave intensities (Fig. 2). The solution of system (2.1), (2.3) is presented as the intersection of cordiform curves (e.g., as the point a_1 of intersection of curves I and II).

The cordiform curves have certain points that correspond to special values of shock-wave intensities. The following values of intensity are special:

— intensity of the normal shock wave

$$J_m(\mathrm{M}_k) = (1+\varepsilon)\mathrm{M}_k^2 - \varepsilon;$$

— intensity of the shock wave decelerating the flow to the critical velocity

$$J_*(\mathrm{M}_k) = (\mathrm{M}_k^2-1)/2 + \sqrt{((\mathrm{M}_k^2-1)/2)^2 + \varepsilon(\mathrm{M}_k^2-1)+1}\,;$$

— intensity of the shock wave with the greatest angle of flow deflection, as compared with all shock waves formed in the flow with a given Mach number

$$J_l(\mathrm{M}_k) = (\mathrm{M}_k^2-2)/2 + \sqrt{((\mathrm{M}_k^2-2)/2)^2 + (1+2\varepsilon)(\mathrm{M}_k^2-1)+2}.$$

In analyzing the differential conditions of compatibility on shock waves [1], the intensities

$$J_p(\mathrm{M}_k) = \frac{3J_m - 2 - 3\varepsilon + \sqrt{9J_m^2 + 2\varepsilon(17+8\varepsilon)J_m + 16 + 16\varepsilon + 9\varepsilon^2}}{2(3+\varepsilon)}$$

(constant-pressure point) and $J_c(\mathrm{M}_k)$ (Crocco point) are identified. The latter intensity is determined by the equation

$$\sum_{n=0}^{3} A_n J_c^n = 0,$$

where

$$A_3 = (1+\varepsilon)(1+3\varepsilon), \qquad A_2 = 4 + 7\varepsilon + \varepsilon^2 - (1+3\varepsilon)J_m,$$

$$A_1 = 1 - 3\varepsilon - (3+3\varepsilon+4\varepsilon^2)J_m, \qquad A_0 = -2(1+\varepsilon J_m).$$

For the intensity $J_i = J_p(\mathrm{M}_k)$, the derivative $\partial \ln p/\partial s$ (flow nonisobaricity) behind the shock wave j_i equals zero. The intensity $J_i = J_c(\mathrm{M}_k)$ corresponds to the zero geometric curvature of the streamline behind the curved shock in a uniform flow. The following inequality is valid for all $\mathrm{M}_k > 1$:

$$1 < J_*(\mathrm{M}_k) < J_c(\mathrm{M}_k) < J_l(\mathrm{M}_k) < J_p(\mathrm{M}_k) < J_m(\mathrm{M}_k).$$

For $\mathrm{M}_k > \sqrt{2}$, we can identify the special intensity

$$J_\Gamma = \mathrm{M}_k^2 - 1$$

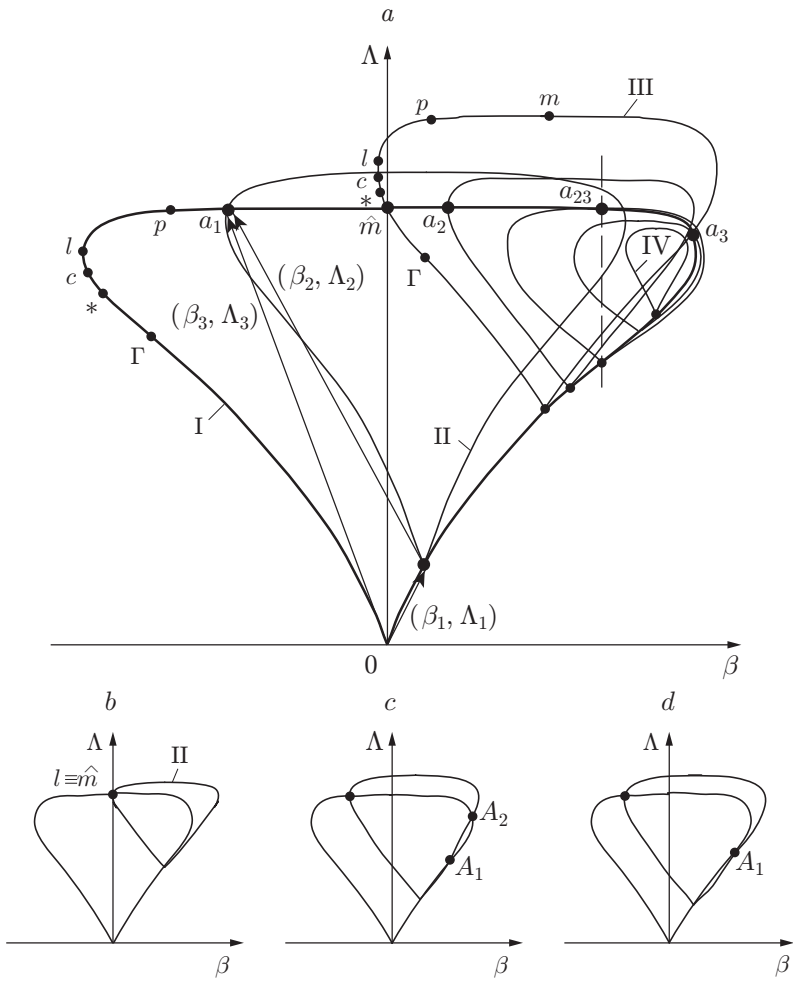

Fig. 2. Triple configurations of shock waves on the plane (β, Λ): (a) general case of the graphic solution with indication of special points on the cordiform curves I and III; (b) formation of von Neumann's SMC; (c) two "alternative" solutions; (d) unique "alternative" solution.

corresponding to the envelope of the family of cordiform curves [10]. The angle of flow deflection on the shock wave with the intensity $J_k = J_\Gamma(\mathrm{M}_k)$ has the maximum value, as compared with all shock waves of the same intensity arising in the flow with different Mach numbers. The flow behind such a shock wave is supersonic [$J_\Gamma(\mathrm{M}_k) < J_*(\mathrm{M}_k)$ and $\mathrm{M}_i > 1$].

Identical special values of intensity are reached on shock waves with the opposite directions of flow deflection. The points Γ, $*$, c, l, p, and m in the cordiform curves I and III (Fig. 2a) indicate the special intensities of shock waves with a negative (clockwise) direction of flow deflection ($\beta_1 < 0$ and $\beta_2 < 0$). Depending on the direction of flow deflection on the shock waves, TCs are classified into the third type [TC-3 ($\beta_1\beta_2 > 0$); Fig. 1a], second type [TC-2 ($\beta_1\beta_2 < 0$ and $\beta_1\beta_3 > 0$); Fig. 1c], and first type [TC-1 ($\beta_1\beta_2 < 0$ and $\beta_1\beta_3 < 0$); Fig. 1e]. The triple configuration with the normal shock j_2 (TCN) formed for $\beta_2 = 0$ (Fig. 1b) and von Neumann's steady Mach configuration with the normal shock j_3 (SMC) formed for $\beta_3 = 0$ (Fig. 1d) are transitional structures between TC-3 and TC-2, TC-2 and TC-1, respectively.

TC-2 is normally formed in the case of irregular (Mach) reflection of the shock wave j_1, whereas TC-1 and TC-3 configurations are usually formed in particular cases of intersection of opposing and overtaking shock waves, respectively. In the case of a subsonic flow behind the shock waves j_2 and j_3, the Mach reflection sometimes leads to formation of configurations of the first or third type [11–13].

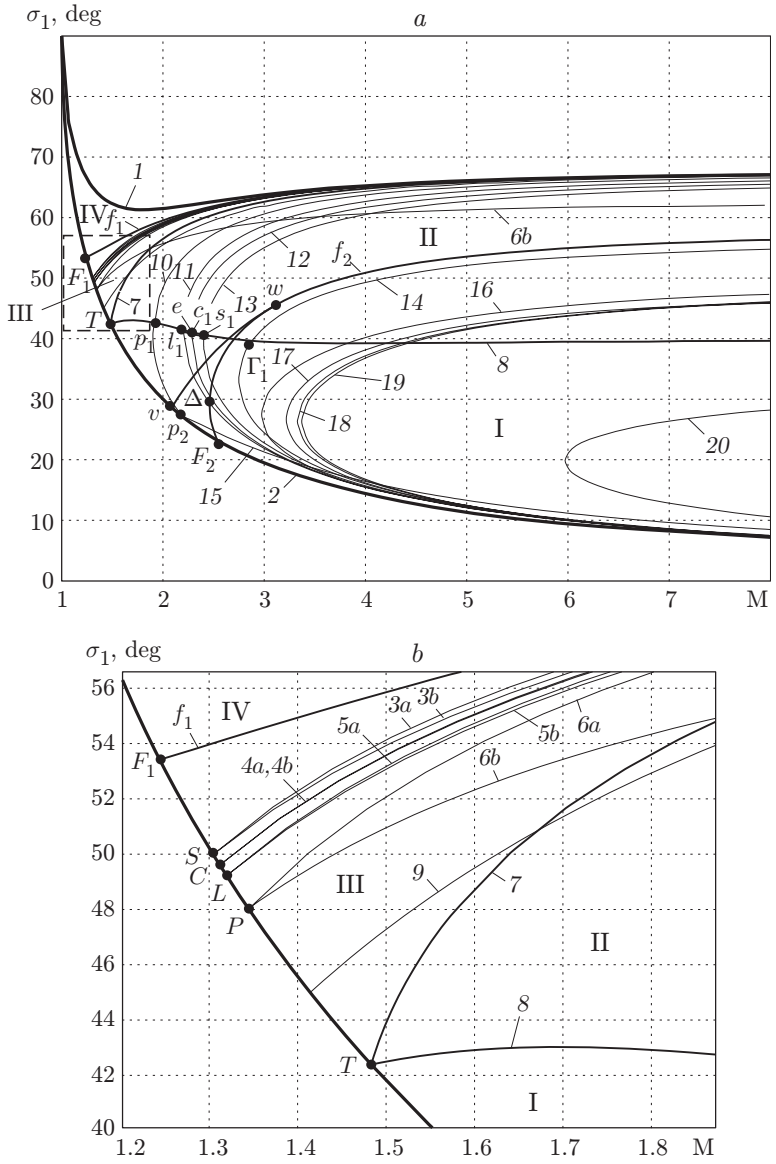

Fig. 3. Special triple configurations of shock waves on the plane (M, σ_1); the zoom-in image of the fragment bounded by the dashed lines in Fig. 3a is shown in Fig. 3b.

The graphic solutions corresponding to TCs of various types are plotted in Fig. 2a by points of intersection of cordiform curves. The points a_i $(i = 1, 2, 3)$ refer to configurations of the ith type, the point a_{23} corresponds to the transitional TCN, and the point $\hat{m}$ of intersection of curves I and III refers to the SMC.

The values of I_f and $\Delta\bar{f}_\tau$ that characterize flow nonuniformity behind the TC are uniquely determined by intensities of the shock waves j_i, the free-stream Mach number, and the ratio of specific heats of the gas. Extreme TCs corresponding to the maximum of nonuniformity parameters are found in the present work for each Mach number of the gas flow.

3. Special Triple Configurations. Triple configurations with the above-noted values (J_m, J_*, J_l, J_p, J_c, and J_Γ) of intensities of individual shock waves are further called the special configurations. The special cases also include the limiting solutions of system (2.1), (2.2) with one of the shock waves degenerating into a weak discontinuity ($J_1 \to 1$ or $J_2 \to 1$). These solutions correspond to the intersection of a shock wave with a weak discontinuity of the same or opposite direction without formation of another (outgoing) weak discontinuity.

As the flow behind the shock wave j_1 is supersonic, the special TCs on the plane (M, σ_1) are sought between curves 1 and 2 (Figs. 3 and 4). The former curve corresponds to the intensity $J_1 = J_*(\mathrm{M})$, and the latter curve refers to degeneration of the shock wave j_1 into a weak discontinuity [$J_1 \to 1$ and $\sigma_1 \to \alpha(\mathrm{M})$, where $\alpha(\mathrm{M}) = \arcsin(1/\mathrm{M})$ is the Mach angle]. In addition, system (2.1), (2.2) has no solution in domain IV between curves 1 and f_1 [1], and no steady TCs are formed. The absence of the solution is shown in Fig. 2a by the nonintersecting curves I and IV. Reflection of shock waves corresponding to domain IV in Fig. 3 is analyzed with the use of a four-wave model [11, 15], which contains an additional expansion wave centered at the point T, and also the model developed in [16] with two tangential discontinuities emanating from this point.

The curves f_i $(i = 1, 2)$ correspond to TC-3 configurations with the shock wave j_2 degenerating into a weak discontinuity $(J_2 \to 1)$. These curves described by the formula [4]

$$\mathrm{M} = \sqrt{[A(B \mp C) - 1 + \varepsilon]/\varepsilon}\,.$$

Here

$$A = (1 + \varepsilon J_1)/[(1 + \varepsilon)(J_1(1 - 3\varepsilon) - 4\varepsilon^2)],$$

$$B = J_1(1 - 2\varepsilon - \varepsilon^2) - 2\varepsilon^2, \qquad C = 2\varepsilon\sqrt{\varepsilon(1 + \varepsilon J_1)(J_1 + \varepsilon)}\,,$$

begin at the points F_i ($\mathrm{M}_{F_1} = 1.245$ and $\mathrm{M}_{F_2} = 2.540$), where

$$\mathrm{M}_{F_{1,2}} = \sqrt{2(1 \pm \sqrt{\varepsilon})/(1 \pm 2\sqrt{\varepsilon}\,)}\,.$$

Domain III contains a unique solution of system (2.1), (2.2), which describes the TC-3. With distance from the curve f_1, the intensity of the shock wave j_2 in TC-3 configurations being formed rapidly increases and consecutively exceeds the special values $J_*(\mathrm{M}_1)$, $J_c(\mathrm{M}_1)$, $J_l(\mathrm{M}_1)$, and $J_p(\mathrm{M}_1)$ on curves 3a–6a (Fig. 3), respectively. The intensity J_3 of the basic shock wave also increases and takes the values $J_*(\mathrm{M})$, $J_c(\mathrm{M})$, $J_l(\mathrm{M})$, and $J_p(\mathrm{M})$ on curves 3b–6b. The intensities of the shock waves j_2 and j_3 in the TC-3 exceed the special value J_Γ: $J_2 > J_\Gamma(\mathrm{M}_1)$ for $\mathrm{M}_1 > \sqrt{2}$ and $J_3 > J_\Gamma(\mathrm{M})$ for $\mathrm{M} > \sqrt{2}$.

TC-3 configurations arising in the case of degeneration of the shock wave j_1 into a weak discontinuity $(J_1 \to 1)$ correspond to the segment F_1T of curve 2 in Fig. 3. The intensities $J_2 = J_3 = J$ of other shock waves in these TCs satisfy the equation

$$\sum_{n=0}^{3} B_n \mathrm{M}^{2n} = 0, \tag{3.1}$$

where

$$B_3 = (1 + \varepsilon)^2 J^2 - 4\varepsilon(J + \varepsilon)^2,$$

$$B_2 = 4\varepsilon(1 - \varepsilon)(J^2 - 1) - 2(1 - \varepsilon^2)J^2(J - 1) - 4(1 - 2\varepsilon)(J + \varepsilon)^2,$$

$$B_1 = (1 - \varepsilon)[4(1 - 2\varepsilon)(J^2 - 1)(J + \varepsilon) + 4(J + \varepsilon)^2 + (1 - \varepsilon)J^2(J - 1)^2],$$

$$B_0 = -4(1 - \varepsilon)^2(J + \varepsilon)(J^2 - 1),$$

which also describes the sequences of shock waves and Prandtl–Mayer waves with extreme values of static pressure behind these shock waves [5].

When the shock wave j_1 degenerates into a weak discontinuity, the intensities of the remaining shock waves are identical $(J_2 = J_3)$ and reach special values simultaneously. Therefore, curves 3a–6a and 3b–6b emanate from the points S, C, L, and P common for the corresponding pairs of curves. The Mach number $\mathrm{M}_S = 1.305$ is determined by the relation

$$4\varepsilon\mathrm{M}_S^6 + (3 + 2\varepsilon - 9\varepsilon^2)\mathrm{M}_S^4 + 4(1 - 8\varepsilon + 6\varepsilon^2)\mathrm{M}_S^2 - 16(1 - \varepsilon)^2 = 0,$$

the value $\mathrm{M}_L = 1.320$ is one of the roots of the equation

$$(1 + 4\varepsilon^2)\mathrm{M}_L^6 - (1 - 2\varepsilon)(1 - 10\varepsilon)\mathrm{M}_L^4 + 8(1 - \varepsilon)(1 - 4\varepsilon)\mathrm{M}_L^2 - 16(1 - \varepsilon)^2 = 0,$$

and the values $\mathrm{M}_C = 1.313$ and $\mathrm{M}_P = 1.345$ are the roots of similar algebraic equations of the seventh and fifth power, respectively.

At the point T [$\mathrm{M}_T = \sqrt{(2-\varepsilon)/(1-\varepsilon)} = 1.483$], the shock waves j_2 and j_3 become normal [$J_2 = J_3 = J_m(\mathrm{M})$], which corresponds to the transition to the TC-2 or TC-1. Curves 7 and 8 (see Figs. 3 and 4) emanating from the point T correspond to the transitional TCN [$J_2 = J_m(\mathrm{M}_1)$] and SMC [$J_3 = J_m(\mathrm{M})$]. The transitional TCN is described by the relation (see [1])

$$\mathrm{M}^4 - r\mathrm{M}^2 + (J_1 - 1)(J_1 + 2 - \varepsilon)/(1-\varepsilon) = 0,$$

where

$$r = (J_1 - 1)(J_1 + 2 - \varepsilon)/(J_1 + \varepsilon) + (J_1 + \varepsilon)/(1 + \varepsilon) + (1 + \varepsilon J_1)^2/[(1-\varepsilon)(J_1 + \varepsilon)^2].$$

The intensity J_3 of the strong [$J_3 > J_l(\mathrm{M})$] shock wave j_3 in the TCN acquires a special value [$J_3 = J_p(\mathrm{M})$] at $\mathrm{M} = \mathrm{M}_a = 1.887$. The branching shock wave j_1 has the intensity $J_1 = J_\Gamma(\mathrm{M})$ at $\mathrm{M} = (1-\varepsilon)\sqrt{2/(1-3\varepsilon)} = 1.667$ [point of intersection of curves 7 and 9 with $J_1 = J_\Gamma(\mathrm{M})$ on the latter]. The shock wave j_2 in the TCN is normal, but the intensity of the shock wave j_1 exceeds J_2 at $\mathrm{M} > 1.645$. Moreover, in the limit ($\mathrm{M} \to \infty$), the intensity of the normal shock j_2 decreases and tends to unity. The intensity J_1 of the branching shock wave is described by the following dependence with accuracy to infinitesimal quantities of order $1/\mathrm{M}^2$:

$$J_1 = \mathrm{M}^2 - 1 + \varepsilon^2 - 2\varepsilon^2/(1-\varepsilon).$$

The same (with respect to M^2) order of special intensities

$$J_*(\mathrm{M}) \to \mathrm{M}^2 - 1 + \varepsilon, \qquad J_{f_1}(\mathrm{M}) \to \mathrm{M}^2 - 1 + \varepsilon$$

shows that domains III and IV for high Mach numbers become infinitely thin on the plane (M, σ_1). The Mach numbers M_i behind all shock waves of this asymptotic TCN tend to unity with accuracy to quantities of a higher order of smallness:

$$\mathrm{M}_1 \to 1 + \varepsilon/[(1-\varepsilon)\mathrm{M}^2], \qquad \mathrm{M}_2 \to 1 + \varepsilon(1-2\varepsilon)/[(1-\varepsilon)\mathrm{M}^2],$$

$$\mathrm{M}_3 \to 1 + (1-2\varepsilon)/[(1-\varepsilon)\mathrm{M}^2].$$

The following relation is valid in the asymptotic TCN:

$$J_3 - J_1 = J_1 J_2 - J_1 = (p_2 - p_1)/p \to 2\varepsilon;$$

it shows that the normal shock j_2 with $\gamma = 1.4$ (see Fig. 1b) increases the static pressure only by 1/3 of the free-stream pressure.

In TC-2 configurations (domain II in Fig. 3a), the intensity of the shock wave j_2 becomes lower than the special values $J_p(\mathrm{M}_1)$, $J_l(\mathrm{M}_1)$, $J_c(\mathrm{M}_1)$, $J_*(\mathrm{M}_1)$, and $J_\Gamma(\mathrm{M}_1)$ on curves 10–14, respectively. The intensity of the shock wave j_2 does not decrease, but the Mach number M_1 in the flow upstream of this shock wave increases. The intensity of the shock wave j_3 also increases and reaches the value $J_m(\mathrm{M})$ on curve 8 (Fig. 3) corresponding to the SMC.

Steady Mach configurations are described by the relation

$$\mathrm{M}^2 = (a_1 + \sqrt{a_1^2 - 4a_0a_2}\,)/(2a_2),$$

where

$$a_2 = (1-\varepsilon^2)(1 + \varepsilon J_1),$$

$$a_1 = (1 + \varepsilon - \varepsilon^2 + \varepsilon^3)J_1^2 + \varepsilon(1 + 3\varepsilon - 2\varepsilon^2)J_1 + (1-\varepsilon)(1+2\varepsilon),$$

$$a_0 = (1-\varepsilon)(J_1 - 1)(J_1^2 + \varepsilon(1-\varepsilon)J_1 - \varepsilon).$$

SMC formation corresponds to the von Neumann criterion of the change in the type of reflection of the shock wave j_1 from the surface. For the smallest value of the Mach number ahead of the SMC ($\mathrm{M} = \mathrm{M}_T$), the intensities of the reflected and basic shock waves are identical [$J_2 = J_3 = 2/(1-\varepsilon) = 2.4$], as well as the values of the Mach numbers

behind these shock waves: $M_2 = M_3 = 1/\sqrt{2}$. As the Mach number ahead of the SMC increases, the intensities J_1 and $J_3 = J_m(M)$ increase monotonically, and the value of J_2 reaches a minimum ($J_2 = 2.278$) at $M = 1.788$.

The reflected shock wave j_2 in the SMC is special at $M = M_{p_1} = 1.908$ [$J_2 = J_p(M_1) = 2.289$], $M = M_{l_1} = 2.202$ [$J_2 = J_l(M_1) = 2.378$], $M = M_{c_1} = 2.287$ [$J_2 = J_c(M_1) = 2.415$], $M = M_{s_1} = 2.404$ [$J_2 = J_*(M_1) = 2.470$], and $M = M_{\Gamma_1} = 2.822$ [$J_2 = J_\Gamma(M_1) = 2.692$]. For the Mach number $M = M_{l_1}$ determined by the equation

$$\sum_{n=0}^{4} C_n M^{2n} = 0$$

with the coefficients $C_4 = (1-\varepsilon)(2-4\varepsilon+2\varepsilon^3-\varepsilon^4)$, $C_3 = -10+20\varepsilon-10\varepsilon^2-10\varepsilon^3+12\varepsilon^4-4\varepsilon^5$, $C_2 = 12-24\varepsilon+10\varepsilon^2+16\varepsilon^3-18\varepsilon^4+6\varepsilon^5$, $C_1 = -2(1+\varepsilon)(3-4\varepsilon+2\varepsilon^2)(1-\varepsilon)^2$, and $C_0 = (1+\varepsilon)(1-\varepsilon)^4$, the SMC simultaneously satisfies another famous criterion of the change in the type of reflection [14] (detachment criterion), which corresponds to the point of tangency of the cordiform curve II of the emanating shock wave and the ordinate axis in Fig. 2b. The Mach number $M = M_{s_1}$ corresponds to the critical velocity of the flow behind the reflected shock wave in the SMC and is the root of the equation

$$\sum_{n=0}^{3} D_n M^{2n} = 0.$$

Here $D_3 = (1-\varepsilon)(1-\varepsilon-2\varepsilon^2+\varepsilon^4)$, $D_2 = -4+6\varepsilon^2-2\varepsilon^3-5\varepsilon^4+3\varepsilon^5$, $D_1 = \varepsilon(4-4\varepsilon-3\varepsilon^2+7\varepsilon^3-3\varepsilon^4)$, and $D_0 = -\varepsilon^2(1-\varepsilon)^3$. At $M = M_e$, the intensities of the incident and reflected shock waves are identical. The point e is determined by the relations

$$M_e = \sqrt{4-3\varepsilon+\varepsilon^2}/(1-\varepsilon) = 2.254, \qquad J_1 = J_2 = 2/(1-\varepsilon). \tag{3.2}$$

At $M > M_e$, the incident shock wave is stronger than the reflected wave. In the limit ($M \to \infty$), it is only the reflected shock wave that has a finite intensity

$$\begin{gathered} J_2 = F(\varepsilon) = (1+\varepsilon-\varepsilon^2+\varepsilon^3+\sqrt{D})/[2\varepsilon(1-\varepsilon)] = 7.271, \\ D = (1+\varepsilon)^2 - \varepsilon(1-\varepsilon)[2(1+\varepsilon)(2-\varepsilon) - \varepsilon^3(1-\varepsilon)], \end{gathered} \tag{3.3}$$

whereas the intensities J_1 and J_3 of other shock waves tend to infinitely high values. The Mach numbers behind the shock waves composing the SMC have finite limits as $M \to \infty$:

$$M_1 = \frac{1-\varepsilon+\varepsilon^2+3\varepsilon^3-2\varepsilon^4+\sqrt{D}}{2\varepsilon(1-\varepsilon^2)} = 5.691, \quad M_2 = 3.506, \quad M_3 = \sqrt{\frac{\varepsilon}{1+\varepsilon}} = 0.378.$$

The Mach number M_2 increases and tends to the above-indicated value, M_3 decreases, and M_1 takes the minimum value ($M_1 = 1.484$) at $M = 1.626$.

In TC-1 configurations (domain I in Fig. 3), the shock wave j_2 has a special intensity [$J_p(M_1)$, $J_l(M_1)$, $J_c(M_1)$, $J_*(M_1)$, and $J_\Gamma(M_1)$] on the lower branches of curves 10–14. The intensity of the strong [$J_3 > J_l(M)$] basic shock wave takes the value $J_3 = J_p(M)$ on curve 15.

Degenerate TC-1 configurations ($J_1 \to 1$) correspond to the segment of curve 1 to the right of the point T (see Fig. 3). Despite the different directions of flow deflection, the intensities $J_2 = J_3 = J$ of the shock waves j_2 and j_3 in these configurations are determined from the same Eq. (3.1) as those in degenerate TC-3 configurations. At $M = M_{p_2} = 2.190$ (point p_2 in Fig. 3), these intensities correspond to the constant-pressure point: $J_2 = J_3 = J_p(M)$.

In addition to the "basic" solution in the domain between the curve vw and f_2 (see Figs. 3 and 4), which is continuous in domains I–III, there are "alternative" solutions of system (2.1), (2.2) for the same values of M and J_1. These solutions describe TC-3 configurations with a supersonic flow behind all shock waves. As the reason for formation of these configurations (interaction of overtaking shock waves) differs from that of formation of the "basic" triple configurations existing at the same values of M and J_1, there are no difficulties in choosing the solution.

"Alternative" solutions arise on the curve vw ($M_v = 2.089$, $M_w = 3.117$, and $J_{1w} = 5.611$) owing to decomposition of the point of tangency of the cordiform curves on the plane of shock-wave intensities. The curvilinear triangle vF_2w contains two solutions of this kind with a non-degenerate ($J_2 > 1$) shock wave j_2 indicated by the points A_1 and A_2 in Fig. 2c. The shock wave j_2 corresponding to one of these solutions (point A_2) degenerates into

a weak discontinuity on the segment F_2w of the curve f_2. As a result, the domain behind the curve f_2 contains the only "alternative" TC-3 (see Fig. 1d) with the shock wave j_2 degenerating on the segment of this curve to the right of the point w. The intensity J_3 of the basic shock wave j_3 in this configuration acquires the special values $J_\Gamma(\mathrm{M})$, $J_*(\mathrm{M})$, $J_c(\mathrm{M})$, $J_l(\mathrm{M})$, and $J_p(\mathrm{M})$ on curves 16–20 (see Fig. 3a), which have horizontal asymptotes.

The coordinates $\mathrm{M}_\Delta = 2.462$ and $J_{1\Delta} = 1.515$ of the extreme left point Δ on the curve f_2 are determined by the equations

$$(1-3\varepsilon)J_{1\Delta}^3 + \varepsilon(1-11\varepsilon)J_{1\Delta}^2 - \varepsilon(4+\varepsilon+9\varepsilon^2)J_{1\Delta} - \varepsilon(1+5\varepsilon) = 0,$$

$$(1-3\varepsilon)^2\mathrm{M}_\Delta^6 - (3-7\varepsilon)(1-2\varepsilon+5\varepsilon^2)\mathrm{M}_\Delta^4$$

$$\ldots + (1-\varepsilon)(3-23\varepsilon+25\varepsilon^2+27\varepsilon^3)\mathrm{M}_\Delta^2 - (1-10\varepsilon-27\varepsilon^2)(1-\varepsilon)^2 = 0.$$

4. Extreme Ratios of Flow Parameters behind the Triple Configurations. The stagnation pressure coefficient I_i (ratio of stagnation pressures behind and ahead of the shock wave j_i) is determined by the intensity J_i as

$$I_i = (J_i E_i^\gamma)^{-(1-\varepsilon)/(2\varepsilon)},$$

where $E_i = (1+\varepsilon J_i)/(J_i+\varepsilon)$ is the ratio of gas densities ahead of the shock wave and behind it in accordance with the Rankine–Hugoniot adiabat. With allowance for the compatibility condition (2.1), the ratio I_{p_0} of stagnation pressures on the sides of the discontinuity τ is

$$I_{p_0} = \frac{p_{02}}{p_{03}} = \frac{I_1 I_2}{I_3} = \Big(\frac{E_3}{E_1 E_2}\Big)^{(1+\varepsilon)/(2\varepsilon)}.$$

The ratios I_f of some other flow parameters f behind the triple configuration have a power dependence on I_{p_0}:

$$I_f = I_{p_0}^\zeta. \tag{4.1}$$

In particular, $\zeta = 2\chi$ [$\chi = \varepsilon/(1+\varepsilon)$] for $f = \rho$ (ratio of gas densities), $\zeta = -2\chi$ for $f = T$ (ratio of temperatures), $\zeta = -\chi$ for $f = a$ (ratio of velocities of sound), and $\zeta = \chi$ for $f = z = \rho a$ (ratio of acoustic impedances at the tangential discontinuity).

The ratios of parameters that explicitly depend on the flow velocity are also determined by the Mach numbers behind the shock waves:

$$I_v = \frac{v_2}{v_3} = \frac{\mathrm{M}_2}{\mathrm{M}_3}\, I_{p_0}^{-\varepsilon/(1+\varepsilon)}, \qquad I_d = \frac{\rho_2 v_2^2}{\rho_3 v_3^2} = \frac{\mathrm{M}_2^2}{\mathrm{M}_3^2},$$

$$I_q = \frac{\rho_2 v_2}{\rho_3 v_3} = \frac{\mathrm{M}_2}{\mathrm{M}_3}\, I_{p_0}^{\varepsilon/(1+\varepsilon)}, \qquad I_w = \frac{p_2+\rho_2 v_2^2}{p_3+\rho_3 v_3^2} = \frac{1+\gamma\mathrm{M}_2^2}{1+\gamma\mathrm{M}_3^2}.$$

Here $q = \rho v$ is the mass flow rate of the gas through a unit surface area, $d = \rho v^2/2$ is the dynamic pressure, and $w = p + \rho v^2$ is the flow momentum.

At the upper boundary (curve f_1 in Fig. 4; $J_2 \to 1$) and the lower boundary (curve 2; $J_1 \to 1$) of domain of existence of the "basic" solution (domain I–III), all the functions considered tend to unity. For each fixed Mach number $\mathrm{M} \geqslant \mathrm{M}_{F_1}$, each of the functions I_{p_0}, I_v, I_q, I_d, and I_w has a unique intensity J_1 of the branching shock wave, which determines the maximum of each function. The parameters of such extreme configurations are shown by curves 9–13 in Fig. 4a and b. It is obvious from Eq. (4.1) that extreme configurations in terms of I_{p_0} also have the maximum ratios of densities and acoustic impedances and the minimum ratios of temperatures and velocities of sound.

For Mach numbers close to M_{F_1}, extreme configurations are TC-3 configurations. As the Mach number increases, TC-2 configurations becomes extreme. The points G_{p_0}, G_v, G_q, G_d, and G_w in Fig. 4b correspond to extreme transitional TCNs. Transitional TCNs are extreme configurations in terms of different ratios of flow parameters behind these configurations at $\mathrm{M} = 1.567$ ($I_v = 1.085$), $\mathrm{M} = 1.569$ ($I_d = 1.201$), $\mathrm{M} = 1.571$ ($I_q = 1.107$), $\mathrm{M} = 1.584$ ($I_w = 1.090$), and $\mathrm{M} = 1.596$ ($I_{p_0} = 1.076$). The intensities J_{1f} of branching shock waves in extreme TC-2 and TC-3 configurations in terms of different ratios I_f satisfy the inequality

$$J_{1v} < J_{1d} < J_{1q} < J_{1w} < J_{1p_0}. \tag{4.2}$$

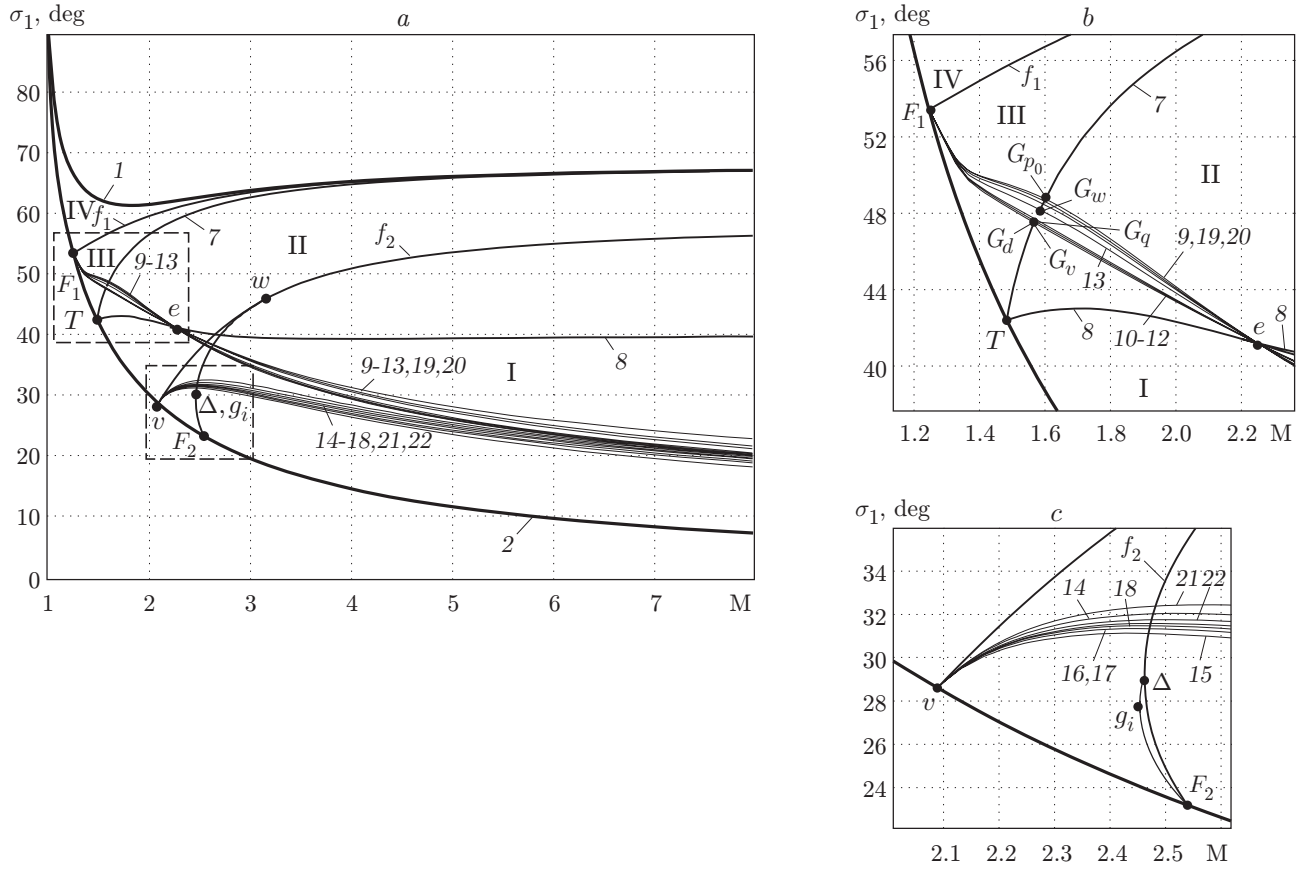

Fig. 4. Extreme triple shock-wave configurations on the plane (M, σ_1): figures (b) and (c) are the zoom-in images of the fragments indicated by the dashed lines in Fig. 4a).

The point e determined by Eq. (3.2) is common for curves 9–13 in Fig. 4a and b and corresponds to the SMC, which is simultaneously extreme in terms of all ratios I_f considered. The extreme SMC satisfies both the condition of the maximum stagnation pressure behind a sequence of two shock waves $\{j_1, j_2\}$ with a fixed product of intensities ($J_1 = J_2$ [2, 3]) and the condition of its minimum behind a single shock wave j_3 [$J_3 = J_m(\mathrm{M})$]. The functions I_f in the extreme SMC take the following values: $I_v = 1.649$, $I_q = 1.833$, $I_d = 3.024$, $I_w = 1.587$, and $I_{p_0} = 1.448$. For $\mathrm{M} > \mathrm{M}_e$, the extreme triple configurations belong to the first type, and the positions of curves 9–13 follow the inequality

$$J_{1p_0} < J_{1w} < J_{1q} < J_{1d} < J_{1v}.$$

Figure 5 shows the ratios of flow parameters behind the extreme and transitional configurations [the scales of the ratio of velocities (curves 2a, 2b, and 2d) are multiplied by 100; the scales of flow-rate functions (curves 3a, 3b, and 3d) and momentum (curves 5a, 5b, and 5d) are multiplied by 10]. In the limit $\mathrm{M} \to \infty$, the ratios I_f of flow parameters behind extreme triple configurations sometimes approach the final values rather slowly (see curves 1a–5a in Fig. 5a):

$$I_{p_0} = \varepsilon^{-(1+\varepsilon)/(2\varepsilon)} = 529.1, \quad I_v = 5.261, \quad I_q = 30.41, \quad I_d = 155.8, \quad I_w = 30.22. \tag{4.3}$$

In extreme configurations in terms of the ratio of stagnation pressures, the shock-wave intensities are describes by the limits

$$\frac{J_1}{\mathrm{M}} \to \sqrt{H}, \qquad \frac{J_2}{\mathrm{M}} \to \sqrt{H}, \qquad \frac{J_3}{\mathrm{M}^2} \to H, \qquad H = \frac{1+\varepsilon-\sqrt{(1-\varepsilon)^2+4\varepsilon^3}}{2\varepsilon(1-\varepsilon)}.$$

In other extreme configurations, the intensities J_1 and J_3 have the order M^2, and the values of J_2 tend to higher but finite limits. Thus, extreme configurations in terms of the ratios of different parameters are different. The values of I_f behind extreme configurations in terms of I_{p_0} only, however, are close to optimal ones (4.3):

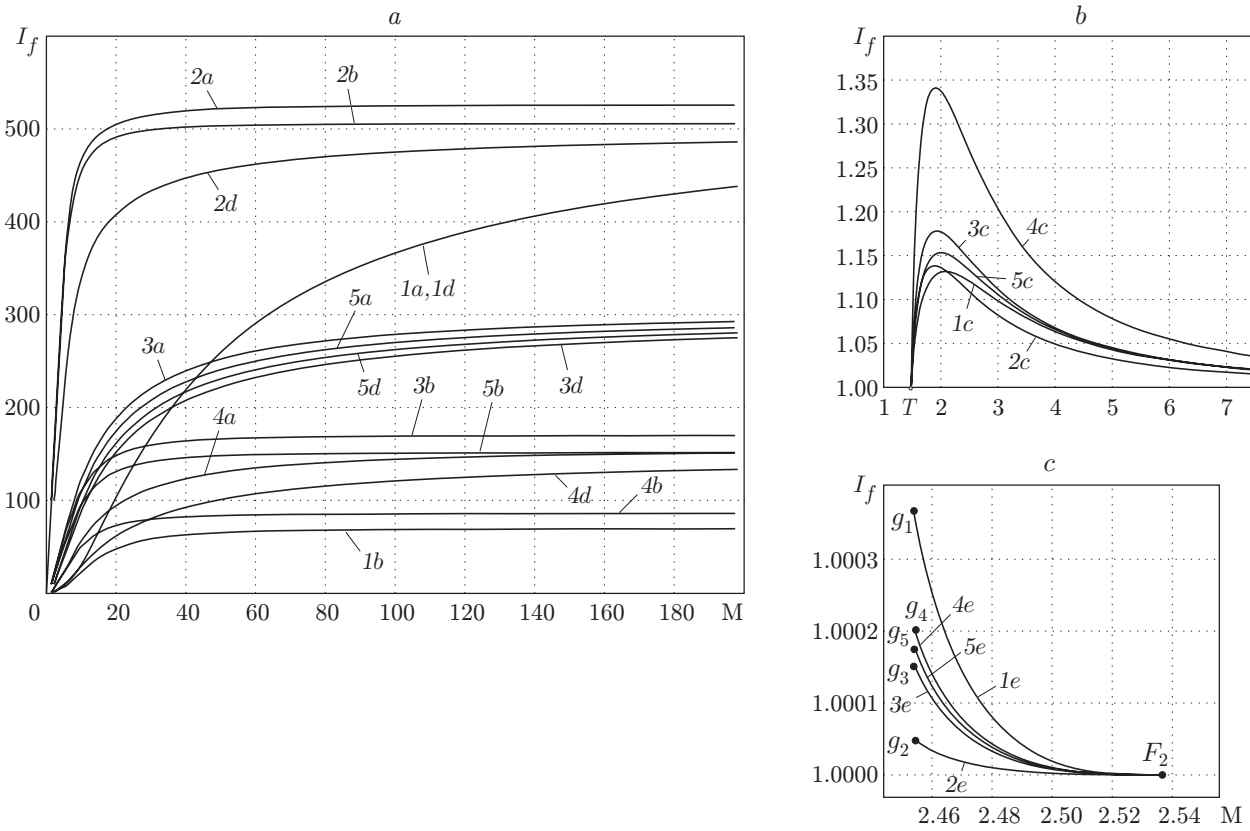

Fig. 5. Ratios of flow parameters behind the extreme and transitional configurations: (a) extreme "basic" and "alternative" configurations (SMC); (b) TCN configurations; (c) "alternative" configurations existing only in the curvilinear triangle vF_2w (see Fig. 4).

$$I_v = \sqrt{\frac{K+N}{2\varepsilon^2}} = 5.033, \qquad I_q = \sqrt{\frac{K+N}{2\varepsilon^4}} = 30.20,$$
$$I_d = \frac{I_v^2}{\varepsilon} = 152.0, \qquad I_w = \sqrt{\frac{K+N}{2\varepsilon^4}} = 30.20. \tag{4.4}$$

Here $K = (1-\varepsilon)^2 + 2\varepsilon^3$ and $N = (1-\varepsilon)\sqrt{(1+\varepsilon)(1-3\varepsilon+4\varepsilon^2)}$.

The ratios of flow parameters behind transitional triple configurations are significantly different from those behind extreme configurations. For instance, they tend to the following values behind the SMC (see curves 1b–5b in Fig. 5a) as $\mathrm{M} \to \infty$:

$$I_{p_0} = \Big(\frac{1+2\varepsilon-2\varepsilon^3+\varepsilon^4+(1-\varepsilon)D}{2\varepsilon(2-\varepsilon)}\Big)^{(1+\varepsilon)/(2\varepsilon)} = 69.72,$$

$$I_v = \sqrt{\frac{(1-\varepsilon)^2+4\varepsilon^3-\varepsilon^4-2\varepsilon^5+\varepsilon^6+(1-\varepsilon)(1-\varepsilon^2)D}{2\varepsilon^2}} = 5.059,$$

$$I_q = \sqrt{\frac{1-2\varepsilon+3\varepsilon^2+\varepsilon^3(1-\varepsilon)^2+(1-\varepsilon)(1+\varepsilon^2)D}{2\varepsilon^4(2-\varepsilon)^2}} = 17.01,$$

$$I_d = \frac{1-2\varepsilon+2\varepsilon^2+2\varepsilon^3-\varepsilon^4+(1-\varepsilon)D}{2(2-\varepsilon)\varepsilon^3} = 86.05, \quad I_w = \frac{1-2\varepsilon+6\varepsilon^2-4\varepsilon^3+\varepsilon^4+(1-\varepsilon)D}{2(2-\varepsilon)\varepsilon^2} = 15.17$$

[the coefficient D was determined by Eq. (3.3)].

In transitional TCNs, the ratios of parameters reach their maximum values ($I_v = 1.138$ at $\mathrm{M} = 1.892$, $I_q = 1.178$ at $\mathrm{M} = 1.927$, $I_d = 1.341$ at $\mathrm{M} = 1.911$, $I_w = 1.153$ at $\mathrm{M} = 2.005$, and $I_{p_0} = 1.132$ at $\mathrm{M} = 2.083$), after which they asymptotically approach unity (curves 1c–5c in Fig. 5b) as a result of degeneration of the shock wave j_2 into a weak discontinuity at high Mach numbers.

TC-3 configurations corresponding to the solution of system (2.1), (2.2), which exists only in the domain to the right of the curves vw and f_2 (see Fig. 4), can also be extreme. The greatest ratios of flow parameters I_{p_0}, I_v, I_q, I_d, and I_w behind these "alternative" TC-3 configurations are reached on curves 14–18 (see Fig. 4), respectively. The positions of these curves in the plane (M, σ_1) satisfy inequality (4.2). The shock-wave intensities in extreme "alternative" TC-3 configurations at high Mach numbers tend to infinite values (J_1 and J_2 tend to values of the order of M, and J_3 tends to values of the order of M^2). The angles β_i of flow deflection in all these TC-3 configurations correspond to the following limits: $\beta_1 \to 0$, $|\beta_2| \to 19.78°$, and $|\beta_3| \to 19.78°$. The extreme ratio of stagnation pressures (curve 1d in Fig. 5a) tends to the same value

$$I_{p_0} = \varepsilon^{-(1+\varepsilon)/(2\varepsilon)} = 529.1, \tag{4.5}$$

as that in the "basic" triple configurations. The maximum ratios of other flow parameters are plotted by curves 2d–5d in Fig. 5a. As $\mathrm{M} \to \infty$, the limits of these ratios coincide with limits (4.4), which are slightly lower than similar values (4.3) for extreme "basic" triple configurations.

Another "alternative" solution of system (2.1), (2.2), which exists only in the curvilinear triangle vF_2w (see Fig. 4), corresponds to TC-3 configurations, which can also be extreme. The maximums of the functions $I_f(J_1)$ are reached at the upper boundary of the domain of existence of this solution (curve vw). The curves $g_i\Delta$ and $g_i f_2$ ($i = 1$–5) in Fig. 4c, which almost merge, characterize the internal local minimums and maximums of the functions I_{p_0}, I_q, I_v, I_d, and I_w, respectively. Local extreme points arise as a result of decay of inflection points of the functions I_f at $\mathrm{M}_{g_1} = 2.453$ (function I_{p_0}), $\mathrm{M}_{g_2} = 2.455$ (function I_v), and approximately identical values $\mathrm{M}_{g_3} - \mathrm{M}_{g_5} \approx 2.454$ (functions I_q, I_d, and I_w). The differences in flow parameters behind the above-described TC-3 configurations at the points of the local maximums are very small (see curves 1e–5e in Fig. 5c). For $\mathrm{M} < \mathrm{M}_{g_i}$, all functions $I_f(J_1)$ increase monotonically from unity at the lower boundary to a certain value at the upper boundary (curve vw) of the curvilinear triangle considered.

The ratios $I_f = f_2/f_3$ of parameters of a nonuniform flow behind the triple configuration do not always give a complete idea of the flow properties. For instance, despite high values of the ratios $I_{p_0} = p_{02}/p_{03}$ (4.5) reached at high Mach numbers, both values p_{02} and p_{03} in these cases are very low as compared to the free-stream stagnation pressure, because the coefficients of stagnation pressure on all shock waves j_i tend to zero.

The TC analysis is supplemented by the study of the differences $\Delta\bar{f}_\tau = (f_2 - f_3)/f$ in flow parameters at the tangential discontinuity τ. Further we consider the functions $\Delta\bar{p}_{0\tau} = (p_{02} - p_{03})/p_0$ and $\Delta\bar{T}_\tau = (T_2 - T_3)/T$; the first of them is the difference in stagnation pressures of two flows and can be used to analyze the emergence of self-oscillatory regimes in jet–obstacle interaction; the second one characterizes the dynamic temperature acting on the mixing layer corresponding to the discontinuity τ.

The functions $\Delta\bar{p}_{0\tau} = I_1 I_2 - I_3 = I_3(I_{p_0} - 1)$ and $\Delta\bar{T}_\tau = \Theta_1\Theta_2 - \Theta_3 = \Theta_3(I_T - 1)$ are equal to zero at the upper boundary (curve f_1 in Fig. 4) and at the lower boundary (curve 2) of the domain of existence of the "basic" solution. Here $\Theta_i = E_i J_i$ is the ratio of gas temperatures on the sides of the shock wave j_i.

For each Mach number $\mathrm{M} > \mathrm{M}_{F_1}$, the domain of existence of the "basic" solution has a unique extreme TC with the maximum differences in stagnation pressure and temperature on the tangential discontinuity behind this configuration. Curves 19 and 20 in Fig. 4a and b show the configurations with the maximum values of $\Delta\bar{p}_{0\tau}$ and $|\Delta\bar{T}_\tau|$. The intensity J_1 of the branching shock wave in extreme configurations in terms of $\Delta\bar{p}_{0\tau}$ can be greater (for $\mathrm{M} < \mathrm{M}_e$) or smaller (for $\mathrm{M} > \mathrm{M}_e$) than that in extreme configurations in terms of the ratios I_f of various parameters f at the discontinuity τ. The transition of extreme TCs of the third type to the second type occurs at $\mathrm{M} = 1.601$, $\sigma_1 = 48.742°$ and $\mathrm{M} = 1.594$, $\sigma_1 = 48.492°$ for stagnation pressures and temperatures, respectively; the transition from the second to the first type occurs at the point e (see Fig. 4b) corresponding to an extreme SMC in terms of all ratios and differences in flow parameters considered.

The value of $\Delta\bar{p}_{0\tau}$ in extreme TCs increases from zero at $\mathrm{M} = \mathrm{M}_{F_1}$ to $\Delta\bar{p}_{0\tau} = 0.423$ at $\mathrm{M} = 3.516$ and then decreases again, tending to zero as $\mathrm{M} \to \infty$ by virtue of high losses of stagnation pressure in shock waves. The extreme difference in temperature $\Delta\bar{T}_\tau$ is negative. It decreases monotonically and unlimitedly as $\mathrm{M} \to \infty$.

"Alternative" TC-3 configurations with extreme differences of stagnation pressures and temperatures at the tangential discontinuity are shown by curves 21 and 22 in Fig. 4a and c. The value of $\Delta\bar{p}_{0\tau}$ in these configurations increases from zero at $M = M_v$ to $\Delta\bar{p}_{0\tau} = 0.423$ at $M = 3.787$ and then decreases again, tending asymptotically to zero. Beginning from $M = 3.661$, the extreme values of $\Delta\bar{p}_{0\tau}$ in "alternative" TCs are higher than those in the "basic" ones. The temperature difference $\Delta\bar{T}_\tau$ is negative and decreases monotonically and unlimitedly but not as fast as in the "basic" triple configurations.

The second "alternative" solution existing only in the curvilinear triangle vF_2w is characterized by insignificant (less than 10^{-4} to 10^{-5}) dimensionless differences in stagnation pressure and temperature of the flow on the sides of the discontinuity τ.

Conclusions. The parameters of a nonuniform flow behind triple configurations of shock waves in a supersonic flow with known gas-dynamic variables are determined (possibly, nonuniquely) only by the intensity J_1 of the shock wave incoming into the triple point. At certain values of the Mach number of the initial flow and intensity J_1, the parameters of flows separated by the slip line (tangential discontinuity) acquire special (e.g., critical) values, and the ratios of some of them have extreme points. Analytical expressions for the special intensities of these incoming shock waves can be used for optimal gas-dynamic design of various engineering objects (supersonic inlets, devices for jet technologies, and rocket launching systems). The optimal design can be aimed at creating or eliminating special and extreme triple configurations and associated self-oscillatory and separated flow regimes.

This work was supported by the Russian Foundation for Basic Research (Grant No. 04-01-00713).

REFERENCES

1. A. L. Adrianov, A. L. Starykh, and V. N. Uskov, *Interference of Steady Gas-Dynamic Discontinuities* [in Russian], Nauka, Novosibirsk (1995).
2. G. I. Petrov, *High-Velocity Aeromechanics and Space Research: Selected Papers* [in Russian], Nauka, Moscow (1992).
3. A. V. Omel'chenko and V. N. Uskov, "Optimal shock-wave systems," *Izv. Akad. Nauk SSSR, Mekh. Zhidk. Gaza*, No. 6, 118–126 (1995).
4. A. V. Omel'chenko and V. N. Uskov, "Optimal shock-wave systems with restrictions on the total angle of flow deflection," *Izv. Akad. Nauk SSSR, Mekh. Zhidk. Gaza*, No. 4, 142–150 (1996).
5. A. V. Omel'chenko and V. N. Uskov, "An optimal shock-expansion system in a steady gas flow," *J. Appl. Mech. Tech. Phys.*, **38**, No. 2, 204–210 (1997).
6. Tao Gang, V. N. Uskov, and M. V. Chernyshov, "Optimal triple configurations of stationary shocks," in: *Proc. of the 24th Int. Symp. on Shock Waves* (Beijing, China, 2004), Vol. 1, Tsinghua Univ. Press, Springer-Verlag, (2005), pp. 499–504.
7. G. F. Gorshkov and V. N. Uskov, "Self-induced oscillations in supersonic jet systems with an impact," *Usp. Mekh.*, **2**, No. 1, 47–67 (2003).
8. K. V. Babarykin, V. E. Kuz'mina, E. A. Ugryumov, and A. I. Tsvetkov, "Self-induced oscillations in an impact of a uniform supersonic flow onto an obstacle consisting of a cylinder and a spike with a disk," *Vestn. St. Peterburg. Univ., Mat., Mekh., Astronom.*, No. 4, 54–64 (2000).
9. A. V. Omel'chenko and V. N. Uskov, "Interference of unsteady oblique shock waves," *Pis'ma Zh. Tekh. Fiz.*, **28**, No. 12, 5–12 (2002).
10. V. N. Uskov, *Shock Waves and Their Interaction* [in Russian], Izd. Leningrad. Mekh. Inst., Leningrad (1980).
11. K. Guderley, *The Theory of Transonic Flow*, Pergamon Press, Oxford (1962).
12. R. Courant and K. Friedrichs, *Supersonic Flow and Shock Waves*, Interscience, New York (1948).
13. L. F. Henderson and A. Lozzi, "Experiments on transition to Mach reflection," *J. Fluid Mech.*, **68**, Part 1, 139–155 (1975).
14. H. G. Hornung, "Regular and Mach reflection of shock waves," *Annu. Rev. Fluid Mech.*, **18**, 33–58 (1986).
15. E. I. Vasil'ev and A. N. Kraiko, "Numerical simulation of diffraction of weak shock waves on a wedge in the von Neumann paradox," *Zh. Vychisl. Mat. Mat. Fiz.*, **39**, No. 8, 1393–1404 (1999).
16. V. N. Lyakhov, V. V. Podlubnyi, and V. V. Titarenko, *Effect of Shock Waves and Jets on Structural Elements* [in Russian], Mashinostroenie, Moscow (1989).